DOI: 10.1002/asia.200700166

Extended Architectures Constructed from Sandwich Tetra-Metal-Substituted Polyoxotungstates and Transition-Metal Complexes

Shou-Tian Zheng,[a] Ming-Hui Wang,[b] and Guo-Yu Yang*[a]

Abstract: Three unprecedented 2D architectures made up of sandwich-type tetra-metal-substituted polyoxotungstates and transition-metal complexes, $[Cu(dien)(H_2O)]_2\{[Cu(dien)(H_2O)]_2[Cu(dien)(H_2O)_2]_2[Cu_4(SiW_9O_{34})_2]\}\cdot 5H_2O$ (**1**; dien = diethylenetriamine), $[Zn(enMe)_2(H_2O)]_2\{[Zn(enMe)_2]_2[Zn_4(HenMe)_2(PW_9O_{34})_2]\}\cdot 8H_2O$ (**2**; enMe = 1,2-diaminopropane), and $[Zn(enMe)_2(H_2O)]_4[Zn(enMe)_2]_2\{(enMe)_2\{[Zn(enMe)_2]_2[Zn_4(HSiW_9O_{34})_2]\}\{[Zn(enMe)_2(H_2O)]_2[Zn_4(HSiW_9O_{34})_2]\}\}\cdot 13H_2O$ (**3**) were hydrothermally synthesized and structurally characterized by elemental analysis, IR spectroscopy, thermogravimetric analysis, and single-crystal X-ray diffraction. Compound **1** consists of anions $[Cu_4(SiW_9O_{34})_2]^{12-}$ linked by copper complexes into a 2D structure, whereas **2** is constructed from novel inorganic–organic hybrid anions $[Zn_4(HenMe)_2(PW_9O_{34})_2]^{8-}$ linked by zinc complexes into a 2D structure. The most interesting is the unique 2D network **3**, which consists of anions $[Zn_4(PW_9O_{34})_2]^{10-}$ with two types of bridging groups: zinc complexes and enMe ligands.

Keywords: coordination polymers · organic–inorganic hybrid composites · polyoxometalates · sandwich complexes · tungsten

Introduction

The preparation of extended polyoxometalate (POM)-based materials is of great interest not only from a structural point of view, but also because of their variety of applications in fields such as catalysis, electrical conductivity, and biological chemistry.[1] However, the technique of linking POM clusters with suitable bridging units to generate extended POM-based solids with desirable properties is in its infancy. An effective method is the reaction of POM cluster units with transition-metal (TM)–organoamine complexes under hydrothermal conditions. This method has been utilized to make many organic–inorganic hybrid extended structures based on polyoxovanadate or polyoxomolybdate clusters, such as $V_{16}O_{38}$,[2] $V_{18}O_{42}$,[3] Mo_8O_{26},[4] $Mo_{12}O_{40}$,[5] $Mo_8V_8O_{44}$,[6] and so on.[7] Typical examples include one-dimensional $[Ni(2,2'\text{-bpy})_2Mo_4O_{13}]$,[4a] $[Cu(enMe)_2]_3[V_{15}O_{36}Cl]\cdot 2.5H_2O$,[7a] and $(H_2en)_2[\{Cu(en)(OH_2)\}Mo_5P_2O_{23}]\cdot 4H_2O$,[7b] two-dimensional $[Co(en)_2][Co(bpy)_2]_2[PMo_8V_8O_{44}]\cdot 4.5H_2O$[6a] and $[M_2(en)_5][\{M(en)_2\}_2V_{18}O_{42}(X)]\cdot 9H_2O$ (M = Zn, Cd; X = H_2O, Cl, Br),[3b] and three-dimensional $[\{Cu(enMe)_2\}_7\{V_{16}O_{38}(H_2O)\}_2]\cdot 4H_2O$[2a] and $[Ni(4,4'\text{-bpy})_2]_2[V_{16}O_{38}Cl](4,4'\text{-bpy})\cdot 6H_2O$[2c] (bpy = bipyridine, en = ethylene diamine). Nevertheless, the synthesis of high-dimensional POM-based solids (2D and 3D) still eludes researchers because it is one of the great challenges facing chemists. The compounds $[Zn_2(en)_5]\{[Zn(en)_2][(bpe)HZn_2As_8V_{12}O_{40}(H_2O)]_2\}\cdot 7H_2O$[8a] (bpe = 1,2-bis(4-pyridyl)ethane), $[Cu_4V_{18}O_{42}(NO_3)(enMe)_8]\cdot 10H_2O$, and $[Cu_4V_{18}O_{42}(SO_4)(enMe)_8]\cdot 10H_2O$[8b] are recent examples. The first is made up of novel arsenic–vanadium clusters linked by the zinc complexes into a 2D framework, whereas the latter two exhibit two rare 3D structures constructed from well-defined $\{V_{18}O_{42}\}$ clusters and copper complexes.

Although many examples of polyoxovanadate/-molybdate clusters linked into 1D, 2D, and 3D materials have already been reported, the linking of polyoxotungstate (POT) clusters with TM–organoamine complexes into extended structures remains largely unexplored, being only recently per-

[a] S.-T. Zheng, Prof. Dr. G.-Y. Yang
State Key Laboratory of Structural Chemistry
Fujian Institute of Research on the Structure of Matter
Chinese Academy of Sciences
Fuzhou, Fujian 350002 (China)
Fax: (+86) 591-8371-0051
E-mail: ygy@fjirsm.ac.cn

[b] Prof. Dr. M.-H. Wang
School of Chemistry and Molecular Engeering
Qingdao University of Science and Technology
Qingdao, Shandong 266042 (China)

Supporting information for this article is available on the WWW under http://www.chemasianj.org or from the author.

formed and restricted to several examples based on $XW_{11}O_{39}$ (X = Cu, Ni)[9] or $W_{12}O_{40}$[10] clusters. For example, Wang and co-workers prepared a unique 3D chiral framework assembled from $W_{12}O_{40}$ clusters and chiral copper complexes.[10a]

The exploration of high-dimensional frameworks based on other POT clusters with metal–organic moieties is therefore attractive. To date, numerous sandwich M_4-substituted POTs, $[M_4(H_2O)_2(XW_9O_{34})_2]^{n-}$ (X = Si, P, As; M = Mn, Fe, Co, Ni, Cu, Zn), have been prepared by conventional solution synthesis at atmospheric pressure and relatively low temperature (below 100 °C).[11] Compared with the above-mentioned well-defined polyoxovanadate/-molybdate clusters, these sandwich M_4-substituted POT anions have a larger volume and a more-negative charge, which allow the formation of higher coordination numbers with TM cations. Hence, these sandwich POT anions may be effective precursors for making high-dimensional solids. However, almost all the reported M_4-sandwiched POTs are, in fact, discrete structures. Although Cronin and co-workers described the first 2D hybrid network constructed from sandwich $[Mn_4(PW_9O_{34})_2]^{10-}$ clusters and sodium complexes quite recently,[12] no high-dimensional framework based on sandwich M_4-substituted POTs and TM complexes have been reported so far. Therefore, the preparation of such solids is an interesting and rewarding challenge. We attempted to make such solids by using trilacunary Keggin XW_9O_{34} (X = Si, P) fragments as precursors under hydrothermal conditions. This is based on the following considerations: 1) hydrothermal-synthesis techniques have been demonstrated to be a powerful tool for making extended POM-based solids,[2–10] 2) our recent work proved that the trilacunary Keggin XW_9O_{34} precursors can exist under hydrothermal conditions and only undergo the isomerization {A-α-XW_9O_{34}}→{B-α-XW_9O_{34}} during the course of the reactions,[13] and 3) under suitable conditions, these precursors have a strong tendency to form dimeric sandwich M_4-substituted POT anions that further act as secondary structural building units. During the course of our investigation, we successfully obtained three inorganic–organic hybrid 2D POMs that involve sandwich M_4-substituted POTs interlinked by TM complexes under hydrothermal conditions: $[Cu(dien)(H_2O)]_2\{[Cu(dien)(H_2O)]_2[Cu(dien)(H_2O)_2]_2[Cu_4(SiW_9O_{34})_2]\}\cdot 5H_2O$ (**1**), $[Zn(enMe)_2(H_2O)]_2\{[Zn(enMe)_2]_2[Zn_4(HenMe)_2(PW_9O_{34})_2]\}\cdot 8H_2O$ (**2**), and $[Zn(enMe)_2(H_2O)]_4[Zn(enMe)_2]_2\{(enMe)_2\{[Zn(enMe)_2]_2[Zn_4(HSiW_9O_{34})_2]\}\{[Zn(enMe)_2(H_2O)]_2[Zn_4(HSiW_9O_{34})_2]\}\}\cdot 13H_2O$ (**3**) (dien = diethylene triamine).

Table 1. Crystallographic data for **1**–**3**.

Compound	**1**	**2**	**3**
Empirical formula	$C_{24}H_{104}Cu_{10}N_{18}O_{81}Si_2W_{18}$	$C_{30}H_{122}N_{20}O_{78}P_2W_{18}Zn_8$	$C_{66}H_{262}N_{44}O_{155}Si_4W_{36}Zn_{18}$
M_r	5942.05	5905.69	12060.82
Crystal system	monoclinic	triclinic	triclinic
Space group	$C2/c$	$P\bar{1}$	$P\bar{1}$
a [Å]	34.240(3)	13.346(3)	17.597(3)
b [Å]	13.360(1)	14.157(4)	18.433(3)
c [Å]	25.166(2)	17.321(5)	19.164(3)
α [°]	90	113.528(4)	91.185(1)
β [°]	109.637(3)	106.4960(10)	107.674(2)
γ [°]	90	90.882(2)	100.775(2)
V [Å^3]	10842.9(14)	2845.9(13)	5798.4(17)
Z	4	1	1
ρ [g cm^{-3}]	3.640	3.446	3.453
μ [mm^{-1}]	21.048	19.883	19.715
$F(000)$	10683	2670	5462
Crystal size [mm^3]	0.35×0.25×0.15	0.10×0.09×0.08	0.23×0.14×0.14
Limiting indices	$-41\le h\le 41$, $-16\le k\le 15$, $-30\le l\le 29$	$-17\le h\le 16$, $-12\le k\le 18$, $-22\le l\le 22$	$-21\le h\le 22$, $-23\le k\le 19$, $-24\le l\le 24$
GOF on F^2	1.071	1.024	1.060
R1,[a] wR2[b] ($I>2\sigma(I)$)	0.0593, 0.1502	0.0368, 0.0865	0.0433, 0.1093
R1,[a] wR2[b] (all data)	0.0657, 0.1556	0.0489, 0.0945	0.0524, 0.1150

[a] $R1=\Sigma||F_o|-|F_c||/\Sigma|F_o|$. [b] $wR2=\{\Sigma[w(F_o^2-F_c^2)^2/\Sigma[w(F_o^2)^2]\}^{1/2}$; $w=1/[\sigma^2(F_o^2)+(xP)^2+yP]$, $P=(F_o^2+2F_c^2)/3$, $x=0.0884$, 0.0535, 0.0597 for **1**–**3**, respectively, and $y=541.8610$, 0.5699, 0.0000 for **1**–**3**, respectively.

Abstract in Chinese:

在水热条件下，首次实现了缺位的钨-氧簇前体与过渡金属配合物间的连接，获得了三个新颖的基于四核过渡金属取代的三明治型钨-氧簇单元通过不同连接方式而构建的无机-有机杂化的二维金属-氧簇网络。化合物 **1** 是基于四核铜取代的三明治型单元$[Cu_4(SiW_9O_{34})_2]^{12-}$通过铜配合物桥连而构建的；化合物 **2** 是基于结构独特的无机-有机杂化的四核锌取代的三明治型单元 $[Zn_4(HenMe)_2(PW_9O_{34})_2]^{8-}$构建的；而化合物 **3** 是非常特别的，它是通过两种不同的桥连基团$[Zn(enMe)_2]^{2+}$和enMe沿不同的方向连接三明治型簇单元$[Zn_4(PW_9O_{34})_2]^{10-}$而形成的新颖的二维层状结构。

Results and Discussion

Crystallographic data for **1**–**3** are presented in Table 1. Selected bond lengths are listed in Table 2. X-ray analysis reveals that the 2D structure **1** is constructed from sandwich Cu_4-substituted polyoxoanions $[Cu_4(SiW_9O_{34})_2]^{12-}$ (**1a**) and copper complexes. As shown in Figure 1a, **1a** is made up of two trilacunary $[B\text{-}\alpha\text{-}SiW_9O_{34}]^{10-}$ moieties linked by four Cu^{2+} ions, which results in a sandwich structure with idealized C_i symmetry. Interestingly, in the central Cu_4 core (Figure 1c and d), the crystallographic independent Cu1 and Cu2 ions exhibit different configurations. Cu2 is bonded to

Table 2. Selected bond lengths (Å) for **1**–**3**.[a]

Bond	1	2	3
W=O_t	1.700(11)–1.743(11)	1.701(6)–1.734(6)	1.705(7)–1.743(6)
W–O_b	1.790(12)–2.235(8)	1.759(6)–2.024(6)	1.771(6)–2.038(6)
W–O_c	2.325(10)–2.407(11)	2.380(6)–2.539(5)	2.299(6)–2.491(6)
Si–O_c	1.623(11)–1.654(10)	–	1.625(6)–1.652(6)
P–O_c	–	1.539(5)–1.558(5)	–

[a] O_t = terminal oxygen atoms, O_b = bridging oxygen atoms bonded to W, Cu, or Zn atoms, O_c = central oxygen atoms bridging Si or P atoms.

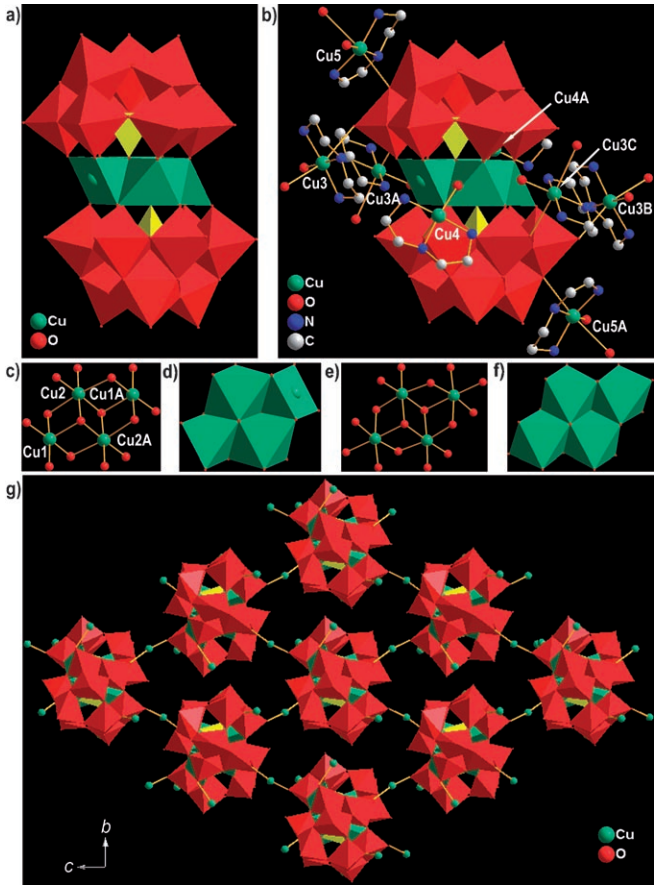

Figure 1. a) Polyhedral representation of polyoxoanion **1a**. b) View of the coordination mode between **1a** and copper complexes. c) and d) Ball-and-stick and poyhedral representations of the central Cu_4 core in **1a**, respectively. e) and f) Ball-and-stick and poyhedral representations of the central M_4 core in reported M_4-substituted POTs, respectively. g) View of the 2D framework of **1** along the *a* axis. All the dien and water ligands are omitted for clarity. WO_6 = red, CuO_5 and CuO_6 = green, SiO_4 = yellow.

six oxygen atoms from **1a** moieties to form a distorted octahedron, whereas Cu1 is defined by five O atoms from **1a** moieties to form a distorted square pyramid. Thus, two CuO_6 octahedra and two CuO_5 square pyramids are linked together by sharing edges to form an unexpected defective rhombic Cu_4 unit, which differs from the usual rhombic M_4 units with four edge-sharing MO_6 octahedra in many reported sandwich M_4-substituted POTs (Figure 1e and f).[11]

Each **1a** moiety acts as an octadentate ligand that coordinates to eight Cu^{2+} ions through six terminal O and two μ_2-O atoms with Cu–O distances of 2.50(1)–2.78(1) Å (Figure 1b). The eight copper ions can be divided into two classes according to their roles as bridging and decorating groups. The bridging groups, which include Cu3 and its symmetry-equivalent atoms Cu3A–Cu3C, are octahedrally coordinated by three equatorial N donors of a dien ligand, one equatorial H_2O molecule, and two *trans*-oxo ligands from two adjacent **1a** clusters. The axial Cu–O bonds (Cu–O: 2.72(1)–2.78(1) Å) are considerably longer than the equatorial Cu–O or Cu–N bonds (Cu–O: 1.95(2) Å; Cu–N: 1.96(2)–2.00(1) Å) owing to Jahn–Teller distortion. On the other hand, the decorating Cu atoms, which include Cu4 and Cu5 and their symmetry-equivalent atoms Cu4A and Cu5A, display two different coordination environments: Cu(4,4A)N_3O_2 square pyramids and Cu(5,5A)N_3O_3 octahedra. The equatorial positions of each CuN_3O_2 square pyramid are occupied by three N atoms from a dien ligand and one water molecule (Cu–N: 1.95(2)–1.99(5) Å; Cu–O: 2.19(1) Å), and the axial position is occupied by one terminal oxo ligand from **1a** clusters (Cu–O: 2.50(1) Å). Similarly, the equatorial plane of the CuN_3O_3 octahedra is defined by three N donors from a dien ligand and one water molecule (Cu–N: 1.93(2)–2.04(2) Å; Cu–O: 2.00(2) Å), but the axial positions are occupied by one terminal oxo ligand and one water molecule (Cu–O: 2.72(3)–2.73(2) Å). Thus, the extended structure of **1** can be described as follows: each **1a** moiety is decorated by two $[Cu(dien)(H_2O)]^{2+}$ and two $[Cu(dien)]^{2+}$ complexes that are not further connected to adjacent **1a** clusters, thus forming a novel tetra-TM-supported polyoxoanion. Furthermore, these TM-supported polyoxoanions are bridged by another four $[Cu(dien)]^{2+}$ complexes through terminal oxo atoms along both the [011] and [01–1] directions with an O–Cu–O angle of 163.1(4)° to form the novel inorganic–organic hybrid 2D framework (Figure 1g). On the basis of bond valence sum (Σs) calculations,[14] the oxidation states of all the Cu, W, and Si atoms are +2 (Σs = 1.61–2.21), +6 (Σs = 5.92–6.29), and +4 (Σs = 3.89), respectively. The oxidation states of these atoms are consistent not only with the overall charge of compound **1**, but also with the reported sandwich Cu_4-substituted POTs.[15]

A noteworthy feature of **1a** is that the absent sites of the unusual defective rhombic Cu_4 units may be good centers for further structural derivation such as intramolecular decoration or intermolecular linkage through organic amine ligands to form novel, unique hybrid structures. For example, two such compounds based on the Zn_4-substituted sandwich anions $[Zn_4(PW_9O_{34})_2]^{10-}$ and $[Zn_4(HSiW_9O_{34})_2]^{10-}$ were successfully synthesized.

The novel 2D structure **2** can be considered to be made up of inorganic–organic hybrid building blocks $[Zn_4(HenMe)_2(PW_9O_{34})_2]^{8-}$ (**2a**; Figure 2a) linked together through zinc complexes. The unique building block **2a** can be derived from the well-known sandwich $[Zn_4(H_2O)_2(PW_9O_{34})_2]^{10-}$ anion[11b] by replacing two water ligands of the central $Zn_4O_{14}(H_2O)_2$ fragment with two enMe ligands (Fig-

CHEMISTRY
AN ASIAN JOURNAL

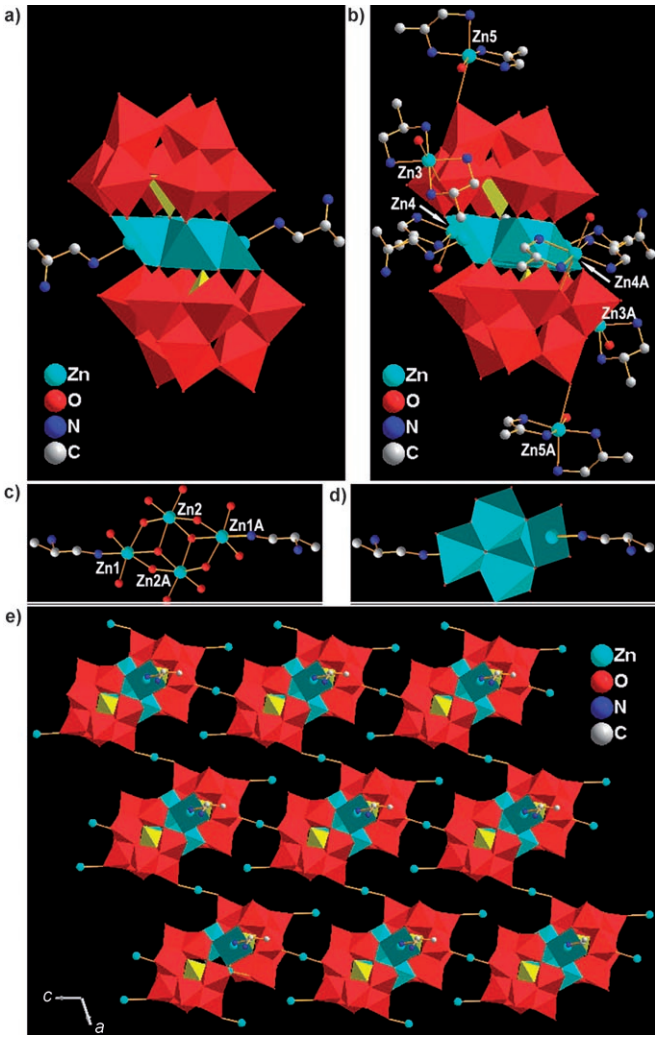

Figure 2. a) Polyhedral representation of polyoxoanion **2a**. b) View of the coordination mode between **2a** and zinc complexes. c) and d) Ball-and-stick and poyhedral representations of the central hybrid Zn_4 core in **2a**. e) View of the 2D framework of **2** along the *b* axis. All the enMe and water ligands are omitted for clarity. WO_6 = red, ZnO_5 and ZnO_6 = green, PO_4 = yellow.

ure 2c and d). Interestingly, both enMe ligands in **2a** serve as monodentate ligands rather than common bidentate chelating ligands; there remains an uncoordinated NH_2 group that is protonated as required by charge-balance considerations. In the $Zn_4O_{14}(HenMe)_2$ fragment, all the Zn centers have a distorted ZnO_6 or ZnO_4N_2 octahedral environment with the Zn–O (2.01(1)–2.33(1) Å) and Zn–N (2.14(1) Å) bond lengths in the usual range. A search of the Cambridge Crystallographic Structure Database (http://www.ccdc.cam.ac.uk) showed that no such hybrid $Zn_4O_{14}(HenMe)_2$ aggregation has been reported so far.

As shown in Figure 2b, each **2a** anion is linked to six Zn atoms through terminal oxo atoms of six WO_6 octahedra to form Zn–O=W interactions. Both crystallographically independent Zn atoms (Zn3 and Zn4), in the bridging role, are octahedrally coordinated with four equatorial N atoms from two chelating enMe ligands (Zn–N: 2.08(1)–2.16(1) Å) and with two axial O atoms from two adjacent **2a** anions (Zn–O: 2.21(1)–2.33(1) Å). On the other hand, the crystallographically independent Zn5 atom takes on the decorating role and also displays octahedral geometry, here defined by one terminal oxo ligand from a **2a** anion, one water ligand, and four N atoms from two enMe ligands (Zn–N: 2.00(1)–2.16(1) Å; Zn–O: 2.48(3)–2.61(1) Å). Thus, each **2a** anion is decorated by two *cis*-$[Zn(enMe)_2O_2]$ groups to form a bi-TM-supported polyoxoanion. These polyoxoanions are then further connected by *trans*-$[Zn(enMe)_2O_2]$ groups along both *a*- and *c*-axis directions to yield another 2D framework based on sandwich POTs (all bridging angles O–Zn–O: 180.0(1)°). On the basis of bond valence sum calculations, the oxidation states of all the Zn, W, and P atoms are +2 (Σs = 1.78–2.03), +6 (Σs = 6.08–6.37), and +5 (Σs = 4.63), respectively. The oxidation states of these atoms are consistent with the overall charge of compound **2**.

The uncoordinated NH_2 groups of the enMe ligands in **2a** suggest that the condensation of **2a** into novel extended solids through the linkage of enMe in an end-to-end fashion could be feasible. A decrease in the initial quantity of enMe resulted in the successful crystallization of solid **3**.

Crystal-structure analysis reveals that the unprecedented 2D hybrid structure **3** is based on two types of distinguishing building blocks, $[\{Zn(enMe)_2\}_2\{Zn_4(HSiW_9O_{34})_2\}]^{6-}$ (**3a**) and $[\{Zn(enMe)_2(H_2O)\}_2\{Zn_4(HSiW_9O_{34})_2\}]^{6-}$ (**3b**), linked by linear enMe ligands to generate a 1D chain, which is extended into a 2D framework by means of the bridging of $[Zn(enMe)_2]^{2+}$ complexes. As shown in Figure 3a and b, although both **3a** and **3b** are bi-zinc-complex-supported polyoxoanions based on $[Zn_4(HSiW_9O_{34})_2]^{10-}$, there are apparent differences between them: 1) both decorating Zn ions of **3a** attach to the anion $[Zn_4(HSiW_9O_{34})_2]^{10-}$ by coordination with the terminal oxo ligands of two W atoms located at equatorial positions, whereas the two decorating Zn ions of **3b** are coordinated to the terminal oxo ligands of two W atoms located at apical positions; 2) both Zn sites (Zn6 and Zn6A) in **3a** have "3+2" trigonal-bipyramidal geometry defined by four N atoms from two enMe ligands and one terminal oxo ligand from **3a** (Zn–N: 2.01(1)–2.11(1) Å; Zn–O: 2.65(1) Å), whereas both Zn sites (Zn5 and Zn5A) in **3b** adopt "4+2" octahedral geometry, with the basal plane defined by the four N atoms of two enMe ligands and the apical positions occupied by one terminal oxo ligand from **3b** and one water ligand (Zn–N: 2.10(1)–2.15(1) Å; Zn–O: 2.21(1)–2.42(1) Å).

In **3**, the building blocks **3a** and **3b** are alternately linked together by linear bidentate enMe ligands through the unique linkage of –enMe–Zn_4O_{14}–enMe–Zn_4O_{14}– to form a 1D chain along the *b* axis (Zn–N: 2.156(11)–2.162(11) Å). Such an unusual linking mode also leads to a hybrid –enMe–Zn_4O_{14}–enMe–Zn_4O_{14}– chainlike structure (Figure 3c and d), which has never been observed to our knowledge, neither in the rich domain of POMs nor in coordination chemistry. Furthermore, adjacent chains of alternate **3a** and **3b** clusters are linked through $[Zn7(enMe)_2]^{2+}$ complexes (Zn–O: 2.30(1)–2.36(1) Å) into a 2D framework

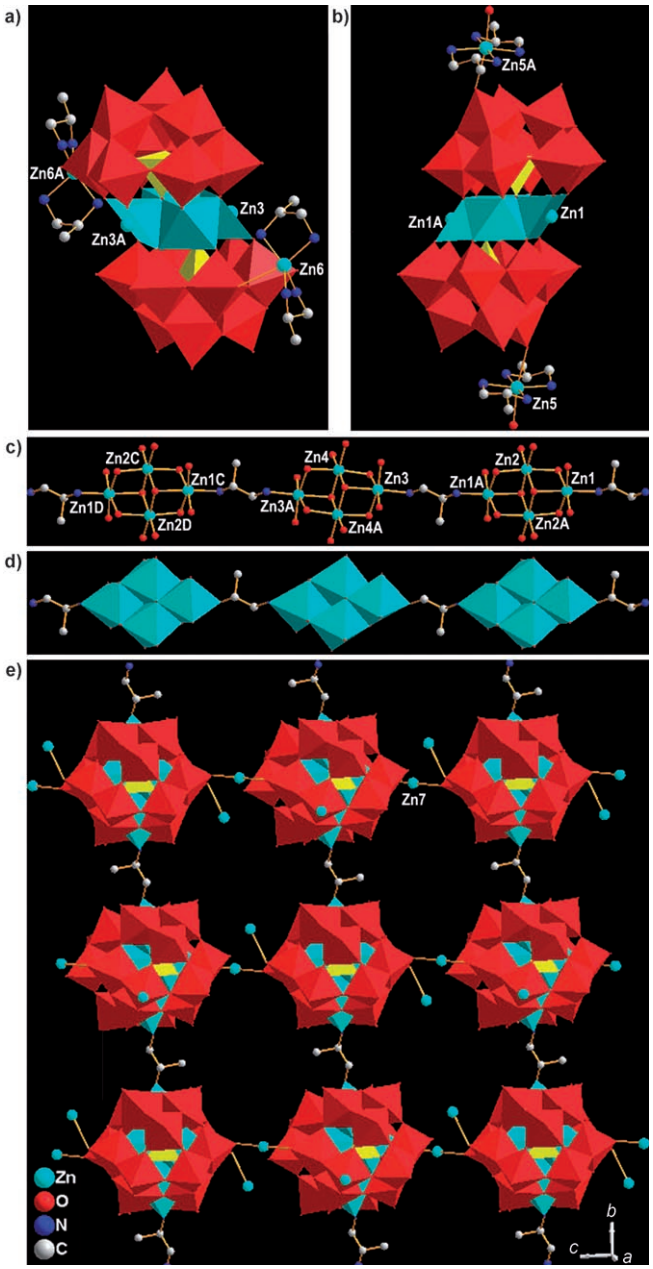

Figure 3. a) and b) Polyhedral representation of polyoxoanions **3a** and **3b**. c) and d) Ball-and-stick and poyhedral representations of the coordination mode between central Zn_4 cores and bridging enMe ligands. e) View of the 2D framework of **3** along the *a* axis. All the water and chelating enMe ligands are omitted for clarity. WO_6 = red, ZnO_5, ZnO_6, and ZnO_5N = green, SiO_4 = yellow.

(Figure 3e), in which each **3a** and **3b** cluster is surrounded by four **3b** and **3a** clusters, respectively. On the basis of bond valence sum calculations, the oxidation states of all the Zn, W, and Si atoms are +2 (Σs = 1.91–2.03), +6 (Σs = 5.98–6.24), and +4 (Σs = 3.82–3.92), respectively. According to the consideration of charge balance, the $[SiW_9O_{34}]^{10-}$ clusters are thus protonated, which is a common feature in many reported POMs.[8a,16]

Notably, in contrast to the neutral 2D frameworks of **1** and **2**, the 2D framework of **3** is anionic. Interestingly, although these three 2D frameworks have remarkable differences, all of them represent a four-connected (4,4) topology by considering the sandwich M_4-substituted POTs as nodes and the bridging TM complexes or linear enMe ligands as links between the nodes.

The stacking of 2D layers of **1**–**3** results in channels along the *c*, *a*, and *a* axes, respectively, which are occupied by lattice water molecules and organic ligands (see Supporting Information, Figures S1–S3). By neglecting all lattice water molecules, calculations[17] show that the effective volumes of the void regions of **1**–**3** are about 1510.8, 356.0, and 593.7 Å^3 per unit cell, respectively, and occupy 13.9, 12.5, and 10.2% of the crystal volumes. Compounds **2** and **3** were selected as examples for thermogravimetric (TG) analysis. As shown in Figure 4, both TG curves show three major weight-loss

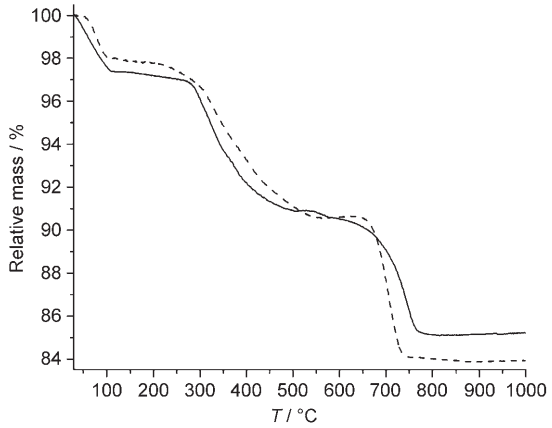

Figure 4. TG curve of **2** (——) and **3** (– – –).

stages, which fall in the regions 34–120, 210–550, and 550–780 °C. The entire weight-loss processes of **2** and **3** are attributed to the loss of enMe ligands and crystal and coordinated water molecules. The observed total weight loss (**2**: 14.93%; **3**: 15.91%) is in agreement with the calculated values (**2**: 15.88%, corresponding to the loss of 11 water and 10 enMe molecules; **3**: 16.63%, corresponding to the loss of 21 water and 22 enMe molecules). Further TG water-sorption experiments were undertaken to study the porosity of **2** and **3**. The TG studies revealed that the crystal water molecules in **2** and **3** can be desorbed by heating a sample at 120 °C to constant weight. Furthermore, the water can be readsorbed by exposing the dehydrated samples to ambient atmosphere for 24 h. The solids **2** and **3** desorbed 3.20 and 3.07% of crystal water, respectively, and within 24 h readsorbed a similar amount of water from the atmosphere. Each procedure was repeated several times to demonstrate the reversibility of the process (Figures 5 and 6). The stability of the materials was also investigated by powder X-ray diffraction, which indicated that the materials retained their crystallinity after several water desorption and readsorption cycles.

CHEMISTRY
AN ASIAN JOURNAL

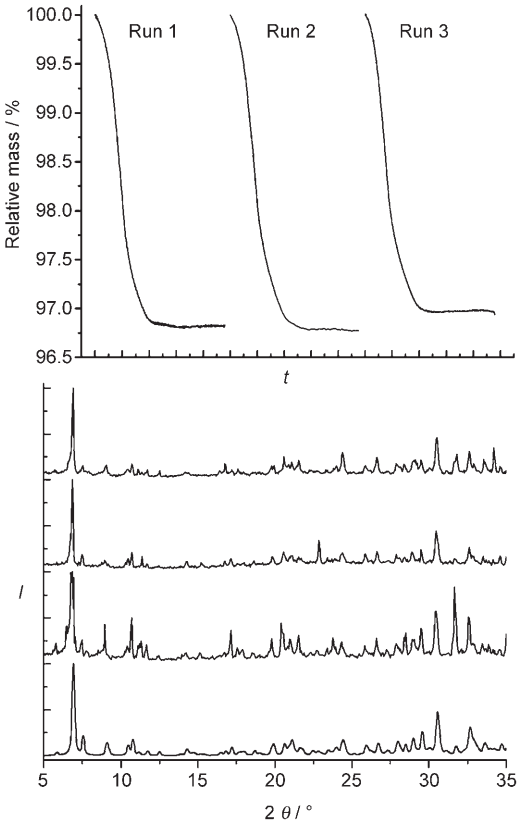

Figure 5. a) TG water-desorption curves of **2** for three consecutive runs. b) Powder X-ray diffraction patterns of **2** (from bottom to top) as simulated from single-crystal XRD, as the native material, after dehydration, and after rehydration (room temperature).

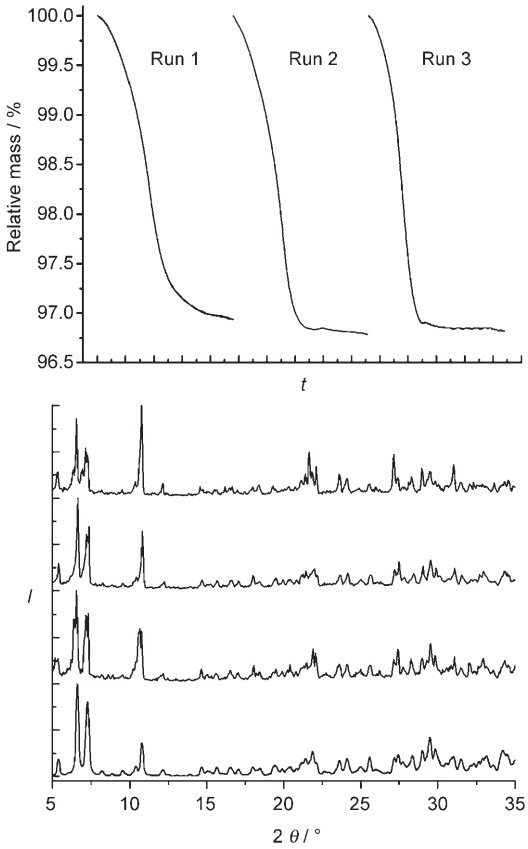

Figure 6. a) TG water-desorption curves of **3** for three consecutive runs. b) Powder X-ray diffraction patterns of **3** (from bottom to top) as simulated from single-crystal XRD, as the native material, after dehydration, and after rehydration (room temperature).

Conclusions

Three novel sandwich M_4-substituted POT-based 2D hybrid materials were synthesized under hydrothermal conditions. These preliminary studies demonstrate the potential of sandwich POTs as molecular building blocks in the construction of novel extended structures, and that the use of hydrothermal techniques is a vital tool for producing extended POM-based solids. It was further shown that these solids exhibit reversible water-sorption capabilities. Further research will concentrate on the suitable modification of the synthetic conditions to synthesize novel sandwich M_4-substituted POT-based 3D architectures with porous properties.

Experimental Section

General

All chemicals employed in this study were of analytical grade and were purchased from commercial sources. Elemental analysis of C, H, and N was carried out with a Vario EL III elemental analyzer. Inductively coupled plasma (ICP) analysis for Cu, Zn, and W were conducted on an Ultima2 spectrometer. IR spectra (KBr pellets) were recorded on an ABB Bomen MB 102 spectrometer. Thermal analysis was performed under dynamic oxygen atmosphere at a heating rate of 10 °C min^{-1} with a METTLER TGA/SDTA851^e thermal analyzer. XRD spectra were obtained on a Philips X'Pert-MPD diffractometer with $Cu_{K\alpha}$ radiation (λ = 1.54056 Å).

Syntheses

1: A mixture of $Na_{10}[A\text{-}\alpha\text{-}SiW_9O_{34}]\cdot nH_2O$ (0.80 g, prepared by literature method[18a]), $CuCl_2\cdot 2H_2O$ (0.17 g), dien (0.10 mL), and H_2O (10 mL) was stirred for 40 min. The pH of this solution was then adjusted from 8.2 to 7.3 by hydrochloric acid (1 mol L^{-1}). Finally, the mixture was transferred to a teflon-lined stainless-steel autoclave (40 mL), kept at 100 °C for 4 days, and then cooled to room temperature. The solid product, which consisted of single crystals in the form of blue blocks, was recovered by filtration, washed with distilled water, and dried in air (0.239 g, 40.4 % yield based on Cu). IR (KBr): 3423 (s), 3212 (s), 2406 (m), 1636 (s), 1398 (s), 1077 (s), 1032 (s), 940 (s), 876 (s), 775 (s), 518 cm^{-1} (m); elemental analysis: calcd (%) for $C_{24}H_{104}Cu_{10}N_{18}O_{81}Si_2W_{18}$: C 4.85, H 1.76, N 4.24, Cu 10.69, W 55.71; found: C 4.76, H 1.93, N 4.11, Cu 10.91, W 55.13.

2: A mixture of $Na_9[A\text{-}\alpha\text{-}PW_9O_{34}]\cdot nH_2O$ (0.80 g, prepared by literature method[18b]), $ZnSO_4\cdot 7H_2O$ (0.20 g), enMe (0.30 mL), and H_2O (10 mL) was stirred for 40 min. The mixture was then transferred to a teflon-lined stainless-steel autoclave (40 mL), kept at 100 °C for 4 days, and then cooled to room temperature. The solid product, which consisted of single crystals in the form of colorless blocks, was recovered by filtration, washed with distilled water, and dried in air (0.194 g, 37.8 % yield based on Zn). IR (KBr): 3423 (s), 3221 (s), 3120 (s), 2937 (m), 1600 (s), 1453 (m), 1379 (w), 1086 (m), 979 (m), 940 (s), 876 (s), 748 (s), 500 cm^{-1} (m); elemental analysis: calcd (%) for $C_{30}H_{122}N_{20}O_{78}P_2W_{18}Zn_8$: C 6.10, H 2.08, N 4.74, Zn 8.86, W 56.05; found: C 6.13, H 2.59, N 4.83, Zn 8.73, W 55.89.

3: A mixture of $Na_9[A\text{-}\alpha\text{-}SiW_9O_{34}]\cdot nH_2O$ (0.80 g), $ZnSO_4\cdot 7H_2O$ (0.20 g), enMe (0.10 mL), and H_2O (10 mL) was stirred for 40 min. The mixture was then transferred into a teflon-lined stainless-steel autoclave (40 mL), kept at 100 °C for 4 days, and then cooled to room temperature. The solid product, which consisted of single crystals in the form of colorless blocks, was recovered by filtration, washed with distilled water, and dried in air (0.157 g, 33.6 % yield based on Zn). IR (KBr): 3414 (s), 3331 (s), 3249 (s), 3148 (s), 2397 (m), 1645 (s), 1581 (s), 1462 (w), 1398 (s), 1068 (s), 986 (m), 940 (s), 872 (s), 757 (s), 528 cm^{-1} (m); elemental analysis: calcd (%) for $C_{66}H_{262}N_{44}O_{155}P_4W_{36}Zn_{18}$: C 6.57, H 2.19, N 5.11, Zn 9.76, W 54.74; found: C 6.46, H 2.33, N 5.01, Zn 9.52, W 54.61.

X-ray Analysis

Crystal-structure determination by X-ray diffraction was performed on a Mercury CCD diffractometer with graphite-monochromated $Mo_{K\alpha}$ ($\lambda = 0.71073$ Å) radiation at room temperature. The program SADABS was used for absorption correction. The structures were solved by direct methods and refined on F^2 by full-matrix least-squares methods with the SHELX97 program package.[19] For **1**, a total of 33278 reflections ($2.36 \leq \theta \leq 25.25°$) were collected with 9512 unique ($R_{int} = 0.0503$), of which 8541 reflections with $I > 2\sigma(I)$ were used for structure elucidation. All non-hydrogen atoms were refined anisotropically. Hydrogen atoms of organic ligands were geometrically placed and refined with a riding model. At convergence, $R1$ ($wR2$) was 0.0593 (0.1502), and the goodness-of-fit was 1.071. The final Fourier map had a minimum and maximum of 6.391 and -3.275 e Å^{-3}. For **2**, a total of 22304 reflections ($2.40 \leq \theta \leq 27.49°$) were collected with 12830 unique ($R_{int} = 0.0289$), of which 10353 reflections with $I > 2\sigma(I)$ were used for structure elucidation. All non-hydrogen atoms were refined anisotropically. Hydrogen atoms of organic ligands were also geometrically placed and refined with a riding model. At convergence, $R1$ ($wR2$) was 0.0368 (0.0863), and the goodness-of-fit was 1.022. The final Fourier map had a minimum and maximum of 2.629 and -1.430 e Å^{-3}. For **3**, a total of 44421 reflections ($2.38 \leq \theta \leq 27.48°$) were collected with 25750 unique ($R_{int} = 0.0412$), of which 21016 reflections with $I > 2\sigma(I)$ were used for structure elucidation. All non-hydrogen atoms were refined anisotropically. Hydrogen atoms of organic ligands were also geometrically placed and refined with a riding model. At convergence, $R1$ ($wR2$) was 0.0430 (0.1080), and the goodness-of-fit was 1.047. The final Fourier map had a minimum and maximum of 3.999 and -3.179 e Å^{-3}. Experimental details for the structure determination of **1–3** are presented in Table 1. Selected bond lengths for **1–3** are listed in Table 2. CCDC-645407–645409 (**1–3**) contain the supplementary crystallographic data for this paper. These data can be obtained free of charge from The Cambridge Crystallographic Data Centre at www.ccdc.cam.ac.uk/data_request/cif.

Acknowledgements

This work was supported by the National Natural Science Fund for Distinguished Young Scholars, 973 Program (No. 2006CB932900), the NSF of China (No. 20473093), the NSF of Fujian Province (No. E0510030), and the Key Project from CAS (No. KJCX2-YW-H01).

[1] a) D. E. Katsoalis, *Chem. Rev.* **1998**, *98*, 359–388; b) J. P. Jolivet, *Metal Oxide Chemistry and Synthesis: From Solution to Solid State*, John Wiley & Sons, New York, **2000**.

[2] a) B. Lin, S. Liu, *Chem. Commun.* **2002**, 2126–2127; b) C. Pan, J.-Q. Xu, G. Li, X. Cui, L. Ye, G. Yang, *Dalton Trans.* **2003**, 517–518; c) S. Liu, L. Xie, B. Gao, C. Zhang, C. Sun, D. Li, Z. Su, *Chem. Commun.* **2005**, 5023–5025.

[3] a) M. I. Khan, E. Yohannes, R. J. Doedens, *Angew. Chem.* **1999**, *111*, 1374–1376; *Angew. Chem. Int. Ed.* **1999**, *38*, 1292–1294; b) M. I. Khan, E. Yohannes, R. J. Doedens, *Inorg. Chem.* **2003**, *42*, 3125–3129.

[4] a) P. J. Zapf, C. J. Warren, R. C. Haushalter, J. Zubieta, *Chem. Commun.* **1997**, 1543–1544; b) D. Hagrman, P. J. Zapf, J. Zubieta, *Chem. Commun.* **1998**, 1283–1284; c) C. Wu, C. Lu, H. Zhuang, J. Huang. *Inorg. Chem.* **2002**, *41*, 5636–5637; d) K. Pavani, S. E. Lofland, K. V. Ramanujachary, A. Ramanan, *Eur. J. Inorg. Chem.* **2007**, 568–578.

[5] a) L. Chong, J. Mao, Y. Sun, J. Song, *Inorg. Chem.* **2004**, *43*, 1964–1968; b) Z. Shi, J. Peng, C. J. Gómez-García, S. Benmansourb, X. Gu, *J. Solid State Chem.* **2006**, *179*, 253–265; c) J. Wang, X. Du, J. Niu, *J. Solid State Chem.* **2006**, *179*, 3260–3264.

[6] a) C. Liu, D. Zhang, M. Xiong, D. Zhu, *Chem. Commun.* **2002**, 1416–1417; b) C. Liu, J. Luo, D. Zhang, N. Wang, Z. Chen, D. Zhu, *Eur. J. Inorg. Chem.* **2004**, 4774–4779; c) Y. Liu, X. Cui, J.-Q. Xu, Y. Lu, J. Liu, Q. Zhang, T. Wang, *J. Mol. Struct.* **2006**, *825*, 45–52.

[7] a) J. R. D. DeBord, R. C. Haushalter, L. M. Meyer, D. J. Rose, P. J. Zapf, J. Zubieta, *Inorg. Chim. Acta* **1997**, *256*, 165–168; b) J. Lu, Y. Xu, N. K. Goh, L. S. Chia, *Chem. Commun.* **1998**, 2733–2734; c) L. Zhang, X. Zhao, J.-Q. Xu, T. Wang, *J. Chem Soc. Dalton Trans.* **2002**, 3275–3276; d) V. Shivaiah, M. Nagaraju, S. K. Das, *Inorg. Chem.* **2003**, *42*, 6604–6606; e) E. Burkholder, S. Wright, V. Golub, C. J. O'Connor, J. Zubieta, *Inorg. Chem.* **2003**, *42*, 7460–7471; f) J. Lu, E. Shen, M. Yuan, Y. Li, E. Wang, C. Hu, L. Xu, J. Peng, *Inorg. Chem.* **2003**, *42*, 6956–6958; g) Z. Kong, L. Weng, D. Tan, H. He, B. Zhang, J. Kong, B. Yue, *Inorg. Chem.* **2004**, *43*, 5676–5680; h) X. Cui, J.-Q. Xu, H. Meng, S.-T. Zheng, G.-Y. Yang, *Inorg. Chem.* **2004**, *43*, 8005–8009; i) S.-T. Zheng, J. Zhang, G.-Y. Yang, *Inorg. Chem.* **2005**, *44*, 2426–2430; j) Y. Lu, Y. Xu, E. Wang, J. Lü, C. Hu, L. Xu, *Cryst. Growth Des.* **2005**, *5*, 257–260; k) L. Chen, X, He, C. Xia, Q. Zhang, J. Chen, W. Yang, C. Lu, *Cryst. Growth Des.* **2006**, *6*, 2076–2085; l) C. Sun, Y. Li, E. Wang, D. Xiao, H. An, L. Xu, *Inorg. Chem.* **2007**, *46*, 1563–1574.

[8] a) Y. Qi, Y. Li, C. Qin, E. Wang, H. Jin, D. Xiao, X. L. Wang, S. Chang, *Inorg. Chem.* **2007**, *46*, 3217–3230; b) Y. Xu, L. Nie, D. Zhu, Y. Song, G. Zhou, W. You, *Gryst. Growth Des.* **2007**, *7*, 925–929.

[9] a) L. Lisnard, A. Dolbecq, P. Mialane, J. Marrot, E. Codjovi, F. Sécheresse, *Dalton Trans.* **2005**, 3913–3920; b) P. Zheng, Y. Ren, L. Long, R. Huang, L.-S. Zheng, *Inorg. Chem.* **2005**, *44*, 1190–1192.

[10] a) H. An, E. Wang, D. Xiao, Y. Li, Z. Su, L. Xu, *Angew. Chem.* **2006**, *118*, 918–922; *Angew. Chem. Int. Ed.* **2006**, *45*, 904–908; b) Y. Ren, X. Kong, X. Hu, M. Sun, L. Long, R. Huang, L.-S. Zheng, *Inorg. Chem.* **2006**, *45*, 4016–4023; c) X. Kong, Y. Ren, P. Zheng, Y. Long, L. Long, R. Huang, L.-S. Zheng, *Inorg. Chem.* **2006**, *45*, 10702–10711.

[11] a) T. J. R. Weakley, H. T. Evans, J. S. Showell, G. F. Tourné, C. M. Tourné, *J. Chem. Soc. Chem. Commun.* **1973**, 139; b) R. G. Finke, M. Droege, J. R. Hutchinson, O. Gansow, *J. Am. Chem. Soc.* **1981**, *103*, 1587; c) S. H. Wasfi, A. L. Rheingold, G. F. Kokoszka, A. S. Goldstein, *Inorg. Chem.* **1987**, *26*, 2934; d) T. J. R. Weakley, R. G. Finke, *Inorg. Chem.* **1990**, *29*, 1235; e) C. J. Gómez-García, E. Coronado, P. Gómez-Romero, N. Casañ-Pastor, *Inorg. Chem.* **1993**, *32*, 3378; f) C. J. Gómez-García, J. J. Borrás-Almenar, E. Coronado, L. Ouahab, *Inorg. Chem.* **1994**, *33*, 4016; g) X. Zhang, G. B. Jameson, C. J. O'Connor, M. T. Pope, *Polyhedron* **1996**, *15*, 917; h) X. Zhang, Q. Chen, D. C. Duncan, C. Campana, C. L. Hill, *Inorg. Chem.* **1997**, *36*, 4208; i) X. Zhang, Q. Chen, D. C. Duncan, R. J. Lachicotte, C. L. Hill, *Inorg. Chem.* **1997**, *36*, 4381; j) J. M. Clemente-Juan, E. Coronado, J. R. Galán-Mascarós, C. J. Gómez-García, *Inorg. Chem.* **1999**, *38*, 55; k) L. Bi, E. Wang, J. Peng, R. Huang, L. Xu, C. Hu, *Inorg. Chem.* **2000**, *39*, 671; l) L. Bi, R. Huang, J. Peng, E. Wang, Y. Wang, C. Hu, *J. Chem. Soc. Dalton Trans.* **2001**, 121; m) U. Kortz, N. K. Al-Kassem, M. G. Savelieff, N. A. A. Kadi, M. Sadakane, *Inorg. Chem.* **2001**, *40*, 4742; n) T. M. Anderson, K. I. Hardcastle, N. Okun, C. L. Hill, *Inorg. Chem.* **2001**, *40*, 6418; o) U. Kortz, I. M. Mbomekalle, B. Keita, L. Nadjo, P. Berthet, *Inorg. Chem.* **2002**, *41*, 6412; p) L. Bi, U. Kortz, B. Keita, L. Nadjo, H. Borrmann, *Inorg. Chem.* **2004**, *43*, 8367; q) X. Fang, T. M. Anderson, C. Benelli, C. L. Hill, *Chem. Eur. J.* **2005**, *11*, 712.

[12] C. Ritchie, E. M. Burkholder, D. L. Long, D. Adam, P. Kögerler, L. Cronin, *Chem. Commun.* **2007**, 468–470.

[13] a) S.-T. Zheng, D.-Q. Yuan, H.-P. Jia, J. Zhang, G.-Y. Yang, *Chem. Commun.* **2007**, 1858–1860; b) S.-T. Zheng, D.-Q. Yuan, J. Zhang, G.-Y. Yang, *Inorg. Chem.* **2007**, *46*, 4569–4574 .
[14] I. D. Brown, D. Altermatt, *Acta Crystallogr. Sect. B* **1985**, *41*, 244.
[15] a) T. J. R. Weakley, R. G. Finke, *Inorg. Chem.* **1990**, *29*, 1235–1241; b) I. M. Mbomekalle, B. Keita, L. Nadjo, K. I. Hardcastle, C. L. Hill, T. M. Anderson, *Dalton Trans.* **2004**, 4094–4095; c) D. Drewes, E. M. Limanski, B. Krebs, *Eur. J. Inorg. Chem.* **2005**, 1542–1546.
[16] a) C. Giménez-Saiz, J. R. Galán-Mascarós, S. Triki, E. Coronado, L. Ouahab, *Inorg. Chem.* **1995**, *34*, 524–526; b) J. Niu, Z. Wang, J. Wang, *Polyhedron* **2004**, *23*, 773–777; c) B. Lin, Y. Chen, P. Liu, *Dalton Trans.* **2003**, 2474–2477.
[17] PLATON program: A. L. Spek, *Acta Crystallogr. Sect. A* **1990**, *46*, 194–201.
[18] a) A. Tézé, G. Hervé in *Inorganic Syntheses*, *Vol. 27* (Ed.: A. P. Ginsberg), John Wiley & Sons, New York, **1990**, p. 87; b) P. J. Domaille, *Inorganic Syntheses*, *Vol. 27* (Ed.: A. P. Ginsberg), John Wiley & Sons, New York, **1990**, p. 100.
[19] a) G. M. Sheldrick, SHELXS97, Program for Crystal Structure Solution, University of Göttingen, Göttingen (Germany), **1997**; b) G. M. Sheldrick, SHELXL97, Program for Crystal Structue Refinement, University of Göttingen, Göttingen (Germany), **1997**.

Received: May 10, 2007
Published online: September 18, 2007

